PAPER

Design of an inchworm actuator based on a ferromagnetic shape memory alloy composite

To cite this article: Yuanchang Liang *et al* 2012 *Smart Mater. Struct.* **21** 115005

View the article online for updates and enhancements.

You may also like

Design of an inchworm actuator based on a ferromagnetic shape memory alloy composite

Yuanchang Liang[1], Minoru Taya[1], John Q Xiao[2] and Gang Xiao[3]

[1] Center for Intelligent Materials and Systems, Department of Mechanical Engineering, University of Washington, Box 352600, Seattle, WA 98195, USA
[2] Department of Physics and Astronomy, University of Delaware, Newark, DE 19716, USA
[3] Micro Magnetics, Inc., Fall River, MA 02720, USA

E-mail: yliang@u.washington.edu

Abstract
A new inchworm actuator has been designed and fabricated based on a ferromagnetic shape memory alloy (FSMA) composite and the hybrid mechanism. The FSMA composite consists of a ferromagnetic material (soft magnet) and a superelastic grade shape memory alloy. The hybrid mechanism is found to provide relatively large force and stroke with fast response on the FSMA composite because it can be driven by a compact electromagnetic driver with high applied magnetic field gradient, providing a large stress capability and reasonably large strain. The inchworm actuator exhibits moderate output force and very large displacement, achieved by accumulating many small strokes based on the inchworm mechanism. The prototype inchworm actuator successfully produces 30 N force and 65 mm s^{-1} stroke velocity.

(Some figures may appear in colour only in the online journal)

1. Introduction

Ferromagnetic shape memory alloys [FSMAs; i.e. iron–palladium (Fe–Pd), nickel–manganese–gallium (Ni–MN–Ga)] have been studied as possible active materials for use in fast response and high power, yet light weight, actuators controlled by a magnetic field [1–3]. There are three mechanisms of actuation associated with FSMAs: (i) magnetic field-induced phase transformation, (ii) martensite variant rearrangement and (iii) a hybrid mechanism. While the first two driving mechanisms of FSMAs produce a very small force [3], the hybrid mechanism can provide large stress capability and reasonably large strain [4]. The hybrid mechanism is based on a sequence of chain reactions: applying a magnetic field with a large gradient, inducing a large stress field in a FSMA actuator material, and promoting stress-induced martensite phase change (austenite → martensite phase); thus, the elastic properties change from stiff austenite phase to soft martensite phase, resulting in large displacement of the FSMA material. Among those FSMAs,

FePd shows promising behavior as an actuator material based on the hybrid mechanism because FePd has both large saturated magnetization and superelasticity [4]. Wada *et al* [5] successfully demonstrated that a FePd helical spring based actuator exhibits a large displacement driven by a compact electromagnetic system. However, FePd is very expensive due to its palladium (Pd) content. Therefore, a FSMA composite was developed as a new and alternative actuator material, which is composed of a ferromagnetic material and a superelastic shape memory alloy (SMA) [6]. A huge force can be induced on the ferromagnetic material such as iron due to the high magnetic field gradient, resulting in a large yet reversible deformation of the superelastic SMA because of the stress-induced martensitic transformation. Among different geometries of FSMA composites, a laminated FSMA composite is easy to make and is most cost-effective without losing its performance. It was successfully demonstrated that a laminated FSMA composite under a high magnetic flux gradient can produce very strong synthetic jet flow and reasonably good power density [7]. Despite the above success,

the order of displacement induced in the FSMA composite membrane actuator is very limited. In order to further increase the stroke of the actuator, the concept of inchworm actuators is examined.

Recently, designs for inchworm linear actuators have been of great interest to both scientific and industrial communities because of their probable superior capabilities of both high force and fast speed. A very informative review has been made by Galantea *et al* [8], where the history of development and the detailed mechanisms of inchworm actuators based on piezoelectric material are presented. Earlier designs of inchworm actuators are used as positioning actuators, for example, in precision machining and tooling which require very large force but limited stroke [9–12]. All of the inchworm actuators developed in the past have two major units, a pusher and a clamper. The basic inchworm mechanism is achieved by rapidly repeating a clamping/releasing and extension/shrinking cycle, resulting in a long stroke that is accumulated in many small steps [8]. Several piezoelectric inchworm actuators have been reported with the aim of increasing the blocking force and stroke [13–19]. Although some of these can reach a relatively high dynamic force of over 100 N, the associated stroke speed is only about several mm s^{-1}. In this study, a novel inchworm actuator based on a laminated FSMA composite is designed with the aim of achieving a higher speed of actuation and larger stroke while maintaining a relatively large blocking force. The design concept is a combination of inchworm motion and a FSMA composite based on the hybrid mechanism. This paper will present the design of the inchworm actuator and its experimental results.

2. Actuator design

Figure 1 shows the sequential movements of the inchworm actuator. The actuator consists of a FSMA composite actuator and a clutch system (figure 1(a)). The FSMA composite will oscillate back and forth, driven by the electromagnetic driver which creates a high magnetic field gradient, while the composite movement will be translated into the linear inchworm motions of the central bar through the clutch system. At t_0 when the FSMA composite actuator is off (figure 1(a)), due to the engaged balls in clutch 1 (the stationary clutch) the central bar cannot move to left. At t_1 when the actuator is turned on (figure 1(b)), the FSMA composite is attracted to the driver while clutch 2 (the active clutch) is moving together with the composite towards to the driver. Therefore, the ball in clutch 2 is engaged with the central bar while that in clutch 1 is disengaged so the bar is no longer controlled by clutch 1. At t_2 in figure 1(c) when the FSMA composite moves further, the central bar moves to the left due to clutch 2 and then completes the first inchworm step. As the drive is turned off at t_3 in figure 1(d), the FSMA composite slides back due to the restoring force of its superelasticity; therefore, clutch 2 moves back to its original position as well. The ball in clutch 2 is disengaged while the ball in clutch 1 is engaged again, resulting in the bar being stationary. In this way, each oscillated motion of
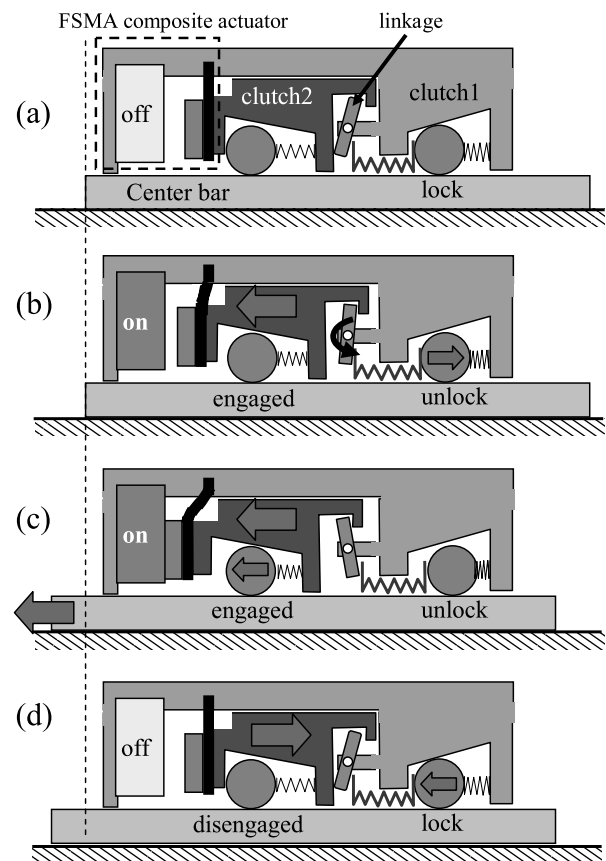
Figure 1. The sequential movements of the central bar in the inchworm actuator from (a) to (d). (a) At t_0, the central bar is stationary and locked by clutch 1. (b) At t_1, the electromagnetic driver is turned on to attract the composite and pulls clutch 2 which locks the central bar. Simultaneously, the bar is released by clutch 1 allowing the bar to move. (c) At t_2, when the composite moves further to left, the central bar moves together with clutch 2. (d) At t_3, the electromagnetic driver is turned off. The FSMA composite springs back and pushes clutch 2 back to the right, resulting in the central bar becoming disengaged. At the same time, the bar is locked by clutch 1.

the FSMA composite can be translated to one step of the linear motion of the central bar. The central bar of the actuator will be the output of the blocking force and displacement of the system. The total accumulated displacement of the bar is determined by the duration of the oscillating FSMA composite. Hence, the inchworm actuator can provide an infinite stroke by accumulating infinite inchworm steps, as long as the length of the central bar is available. The two-way direction of the bar's movement can be easily realized by adding an identical system to figure 1(a) which is just a mirror image of the right actuator system.

The mechanism of the clutch system is schematically shown in figure 2. When the clutch moves to the left as one inchworm step, the ball will engage both the inclined clutch inner surface and the rod surface, resulting in the rod moving in the same direction together with the clutch (figure 2(b)). When the clutch moves to the right after the end of an inchworm step, the ball will no longer engage with both the clutch and the rod, so the rod will be stationary while the
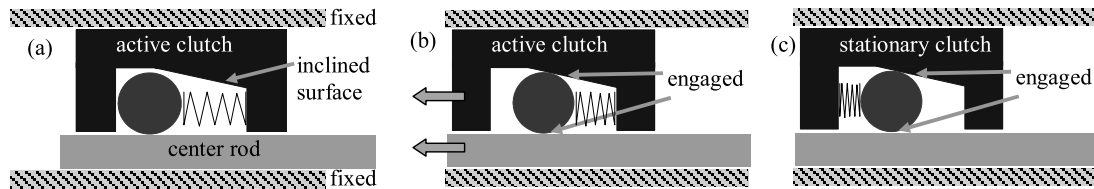
Figure 2. Schematic of the inchworm mechanism of the clutch system (a) before actuation and (b) after actuation, and (c) the stationary clutch.
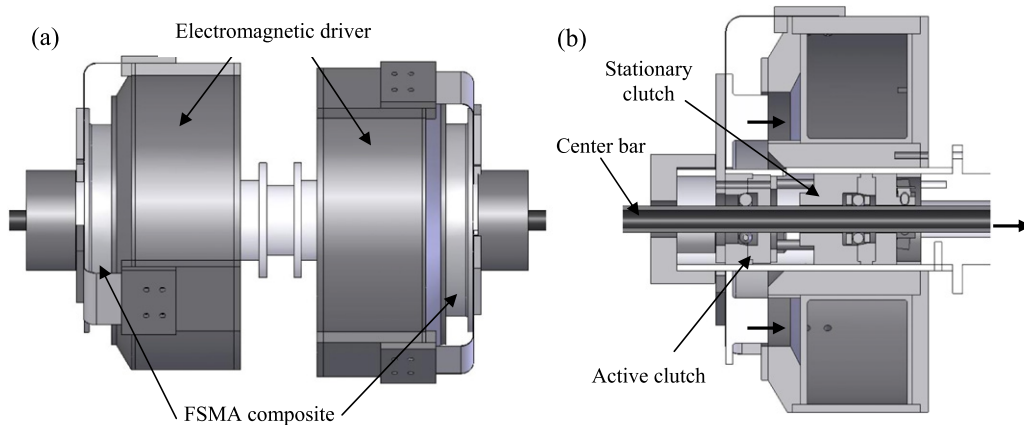
Figure 3. (a) Schematic of the two-way inchworm actuator based on a FSMA composite membrane. (b) Cross-sectional view of the left side, where the arrows show the direction of movement of the FSMA composite and the central bar when the driver is on.
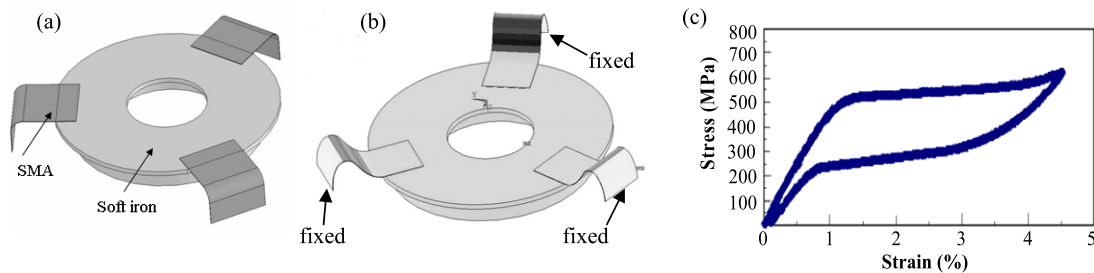
Figure 4. (a) Schematics of the FSMA composite membrane, (b) its simulated deformation by finite element analysis (FEA), and (c) the tensile stress–strain curve of the superelastic grade NiTi plate.

clutch returns to its original position. This is called the active clutch. In addition, if the clutch is stationary and a spring is attached to the ball so that the ball always engages to the clutch and the rod, then the rod cannot move in any direction, figure 2(c). This is called the stationary clutch. Both active and stationary clutches are used in the present inchworm actuator, where clutch 2 is active and clutch 1 is stationary as shown in figure 1.

Figure 3 shows the two-way design of the FSMA composite inchworm actuator which consists of two identical one-way inchworm actuators. Each one-way actuator consists of three sub-systems: (i) the FSMA composite, (ii) the electromagnetic driver; and (iii) the clutch system (figure 3(b) is a cross-sectional view of the left part of figure 3(a)). The FSMA composite will oscillate back and forth driven by the electromagnetic driver, where oscillations will be translated into linear inchworm motions by the active clutch. When the actuator is inactivated, both the stationary clutches hold the central bar and provide the blocking force so the bar cannot move in either direction. As the arrows show in figure 3(b), when the left driver is turned on, the FSMA composite will be attracted to the right, resulting in the central bar being pushed to the right. The FSMA composite membrane consists of three superelastic L-shaped SMA plates made of nickel–titanium (Ni–Ti) and a ferromagnetic soft iron ring (figure 4(a)), where the overall diameter is 125 mm. The thickness of the L-shaped SMA plate is 0.2 mm and the width is 24 mm. The L-shape can be formed by shape memorizing a straight thin plate with the desired dimensions ($0.2 \times 24 \times 70.85$ mm in the present case). Heat treatment for the shape memorizing process is at 510 °C for 5 min followed by the water quenching. The FSMA composite is clamped on SMA components along the outer circumference of the composite (figure 4(b)), while the inner circumference is able to freely slide on the outer circumference of the housing. The superelastic loop of the tensile stress–strain curve of NiTi is characterized as shown in
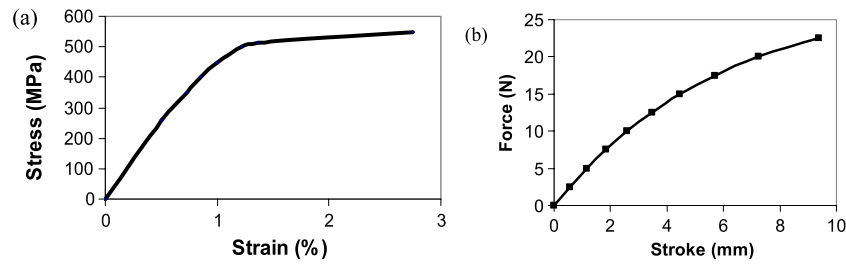
Figure 5. (a) The input material data for FEA analysis, and (b) the predicted force–displacement curve of the FSMA composite in figure 4(b).
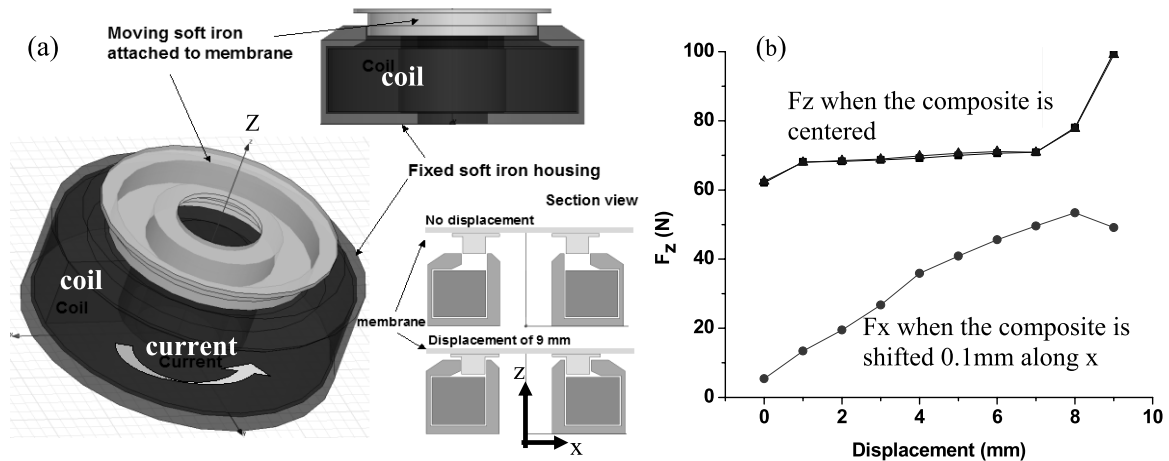
Figure 6. (a) Schematic of the electromagnetic driver and (b) its estimated performance.

figure 4(c). This sliding motion of the composite membrane is activated by the electromagnetic driver which creates a high magnetic field gradient around the soft iron ring. As the driver is turned on and the iron ring is attracted, the thin SMA plate bends and the FSMA composite slides forward. As the driver is turned off, the FSMA composite slides back due to the restoring force of the superelastic SMA component.

In order to estimate the deformation of the FSMA composite, ANSYS finite element analysis (FEA) was performed as shown in figure 4(a), which displays a model of the composite with an overall diameter of 123 mm and height of 13 mm. The SMA is made of superelastic grade NiTi and its nonlinear loading curve (figure 5(a)) is used as the input data for the FEA analysis, where the curve is approximated from the loading curve in figure 4(c). The predicted quasi-static deformation and the estimated force–displacement (*F*–*D*) curve are shown in figures 4(b) and 5(b), respectively. The *F*–*D* curve exhibits nonlinear behavior due to the superelasticity of the SMA. The resonance frequency of the FSMA composite, including the weight of the activated clutch, is estimated as 18 Hz. Based on the frequency response of the FSMA composite, the first mode of vibration at the resonant frequency can be utilized to enhance the system performance, i.e. reducing the consumption of the input power while increasing the efficiency.

Several designs of electromagnetic drivers were explored, including different geometries and arrangements between the yoke of the driver and the soft iron of the FSMA composite.

The electromagnetic force of each design was estimated by the numerical simulation software, Maxwell 3D. The optimized geometry of the electromagnetic driver to provide a high magnetic field gradient is shown in figure 6(a), where the overall diameter is about 120 mm and the height is 47 mm. It is designed to provide a constant force by a given electrical current while the FSMA composite is attracted and moves within a 9 mm stroke as shown in the section view of figure 6(a). The estimated performance of the FEA is shown in figure 6(b) where the 1.5 A mm^{-2} electrical current density and the 0.8 filling factor of the electrical coil winding are used. The driver is expected to induce a force of about 70 N (Fz) when the FSMA composite is moving from 0 to 9 mm where the *z*-axis is defined in figure 6(a). If the FSMA composite is slightly off-center, the side force (Fx) is also estimated, where the *x*-axis is defined in figure 6(a). It is shown in the figure 6(b) that Fx increases as the membrane moves from 0 to 9 mm, resulting in increasing friction as high as 50 N on the interfaces between the membrane and the electromagnet when the FSMA composite is slightly off-center by 0.1 mm. Therefore, it is very important to ensure that the FSMA composite is well-centered. For the prototype, a Teflon ring is attached as a spacer between the membrane and the electromagnet to reduce the friction.

3. Test results for the prototype actuator

The prototype of the two-way inchworm actuator is shown in figure 7(a). The overall size without the central bar is
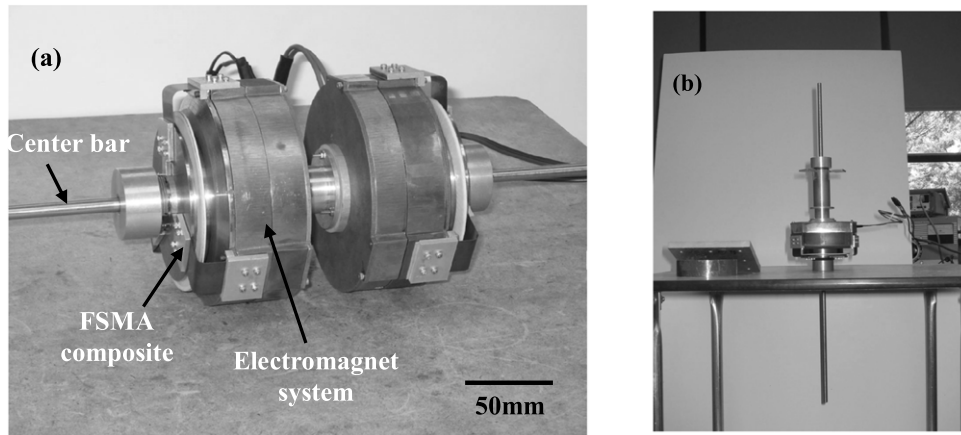
Figure 7. (a) Photo of the two-way inchworm actuator. (b) The one-way actuator system.
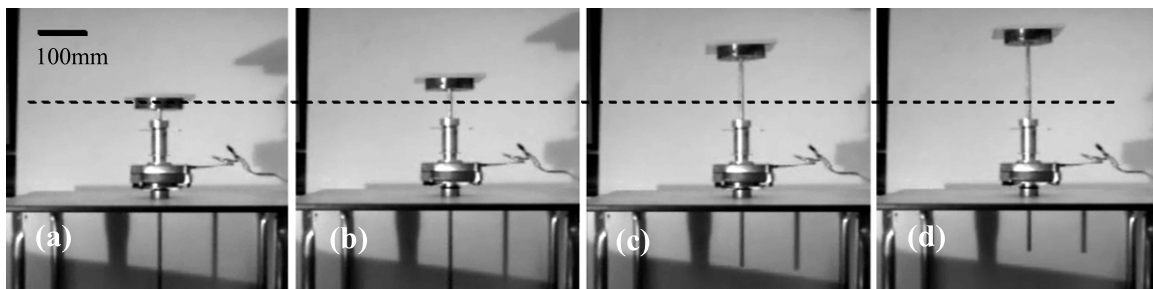
Figure 8. Sequential photos of the one-way actuation in the vertical direction.
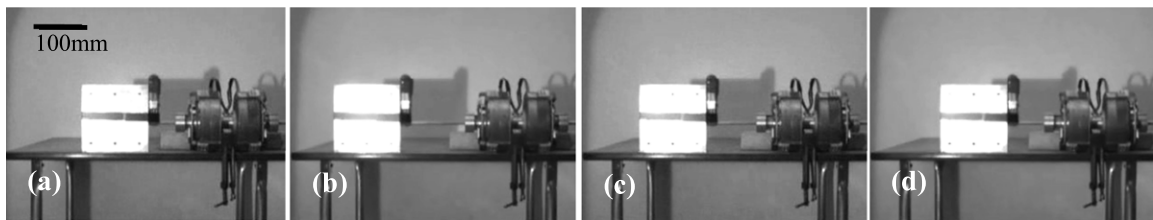
Figure 9. Sequential photos of the two-way actuation in the horizontal direction.

125 mm in diameter and 210 mm in length, and the total weight is about 8.2 kg. The electrical resistance of each coil is about 0.42Ω. The FSMA composite is driven by the electromagnetic driver based on the hybrid mechanism. The hybrid mechanism is based on a sequence of chain reactions: an applied large magnetic field gradient induces a large stress field in a FSMA actuator material, prompting a stress-induced martensite phase change (austenite → martensite phase), leading to a change in the elastic properties from stiff (austenite phase) to softer (martensite phase), resulting in a large displacement. Then, the force and the stroke are transferred to the central bar via the active clutch, where central bar provides actuation power out of the system. The speed of the inchworm motion can be very fast when the FSMA composite is driven at a high frequency. The inchworm actuator can also be used for one-way actuation as shown in figure 1(b) where the weight is about 4.1 kg and the length of the one-way actuator is half that of the two-way actuator.

Figures 8 and 9 demonstrate the test results for the actuator. The one-way actuator is positioned vertically as shown in figure 8(a) where a 3 kg block is on the top of the central bar. As the actuator is switched on, the electromagnetic driver is powered by a pulse wave voltage generated by a power amplifier connecting to a DC power supply, where the frequency of the pulse wave is adjustable. The block will be pushed up against gravity figures 8(b)–(d). When the actuator is turned off, the block will stay still because the central bar is locked by the stationary clutch inside the actuator to prevent the bar from free falling. Due to the limited length of the central bar, the total accumulated displacement of the block in figure 8(d) is 240 mm, where the displacement of one completed inchworm step is about 10 mm. The block can be much higher if a longer central bar is available. Additionally, the 3 kg block moves smoothly upward at a speed of 65 mm s^{-1} when the actuator is driven at 14 Hz. A similar moving speed can be obtained by a lower frequency such as 7 Hz because each stroke of the actuator at 7 Hz

Table 1. Comparisons of inchworm actuator performance parameters.

	Dynamic loading (N)	Speed (mm s^{-1})	Maximum stroke (mm)	Frequency (Hz)	Weight (kg)	Volume (cm^3)
Galantea *et al* [8]	50	10	10	300		48
Tenzer *et al* [9]	40	2.2	Positioner	320	0.45	100
Le Letty *et al* [10]	37	23	10	2250	0.5	270
Zhang *et al* [11]	200	6	Positioner		0.7	
May [12]	20	2	Positioner		0.3	
Kim *et al* [15]	9	0.93	Infinite	20		
Vaughan [16]	90	5	Infinite	50		
Li *et al* [17]	40	6	Infinite	12		48
Frank *et al* [18]	150	1	Infinite	150		60
Newton *et al* [19]	1	0.18	Infinite	500		
The present work	30	65	Infinite	14	4.1	1250

is larger than the one at 14 Hz due to the response of both the clutch system and the electromagnetic driver, but the movement at lower frequency is not as smooth as a higher frequency. The two-way actuation of the actuator system which is positioned horizontally is shown in figure 9. The actuator has two sets of electromagnetic drives and FSMA composites which are in mirror positions to each other with respect to the mid point; therefore the actuator can provide two-way actuation where the block is pushed to the left (figures 9(a) and (b)) and pulled to the right (figures 9(c) and (d)) when the right and the left halves of the system are switched on and off, respectively. High speed movement of the block is also successfully demonstrated when the two-way actuator is driven by the power amplifier controller at a higher frequency. Although the FSMA composite based inchworm actuator provides a moderate blocking force of 30 N, the stroke speed is very fast as shown in table 1 when the performance of this actuator is compared with that of the past inchworm actuators based on piezoelectric materials.

4. Discussion

The loading–unloading curve of the FSMA composite membrane is obtained with an Instron tester as shown by the black dots in figure 10, where the composite is made of superelastic NiTi and soft iron figure 10. The hysteresis loop of the curve is due to the superelastic property of NiTi. The curve shows that the stress-induced martensitic (SIM) phase transformation of NiTi starts at the stroke of 3.5 mm. The estimated loading curve of the FSMA composite (solid line in figure 10) is in a good agreement with the experimental result. The maximum oscillating stroke of the FSMA composite occurs at 14 Hz which is less than the predicted value (18 Hz). This is due to the additional mass of the 3 kg block as shown in figure 7 and the friction between the composite membrane and the housing. The friction could be reduced by using better lubrication. If a higher actuation speed is desired, the resonance frequency of the FSMA composite can be made higher by stiffening the composite structure, for example by using a thicker NiTi plate.

The test results show that the maximum lifting force of the inchworm actuator is about 3 kg at a stroke speed of 65 mm s^{-1}. The force is much less than the expected
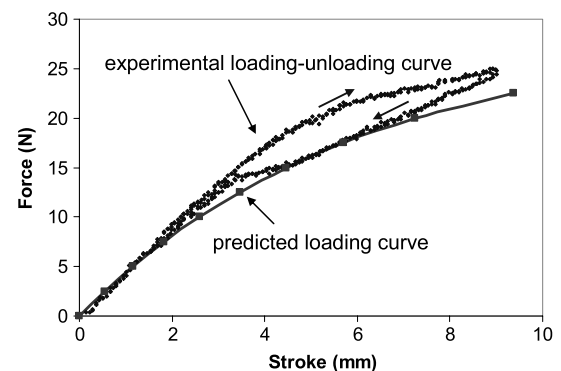
Figure 10. Experimental (black dots) and estimated (solid line) force–displacement curves of the FSMA composite.

value of 7 kg as shown in figure 6(b). The reasons why there is a difference of over 50% between the experimental and estimated results are twofold. The first is on the soft iron material of the electromagnetic driver. Figure 11(a) shows two magnetization curves of soft iron and LVT steel, where the soft iron is used in the prototype system and the laminated LTV steel (made by the Ling–Temco–Vought (LTV) Corporation) is used in the estimation. The initial slope of the magnetization curve (i.e. *M–H* curves) for soft iron is much less than that for laminated LTV steel, although their saturated magnetizations are almost the same. The initial difference in their *M–H* curves gives a large gap between the tested and the estimated results as shown in figure 11(b). After using the corrected magnetization curve, the estimated force is close to the tested value (black square and gray triangle lines).

The second reason is due to the activation of the active clutch system which moves together with the FSMA composite, as shown in figures 2(a) and (b). During the dynamic tests of the inchworm actuator, the clutch balls cannot fully engage the central bar when the actuation frequency increases, therefore slippage between the activated clutch and the rod occurs. This is because the clutch balls cannot move back and forth fast enough as the frequency increases to engage and release the central rod in order to complete one inchworm step. Currently, a rubber ring is placed between the balls and the clutch as a mass–spring
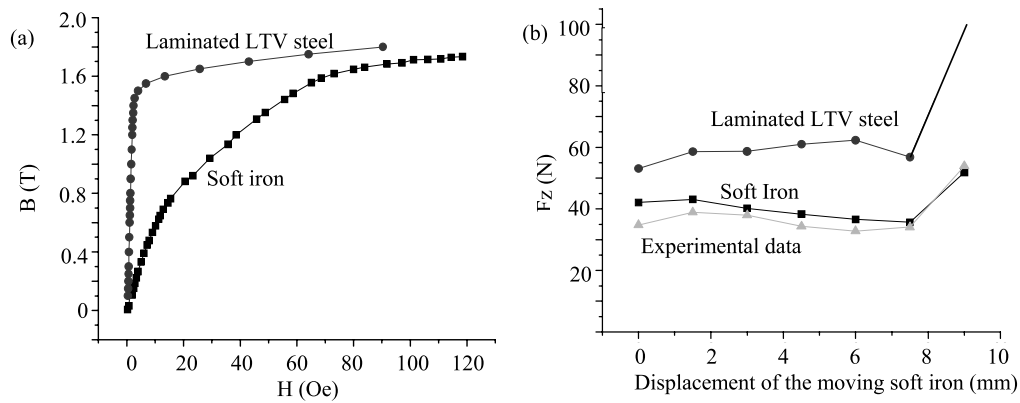
Figure 11. (a) The magnetization curves of soft iron and laminated LTV steel. (b) Comparisons of estimated and tested forces.
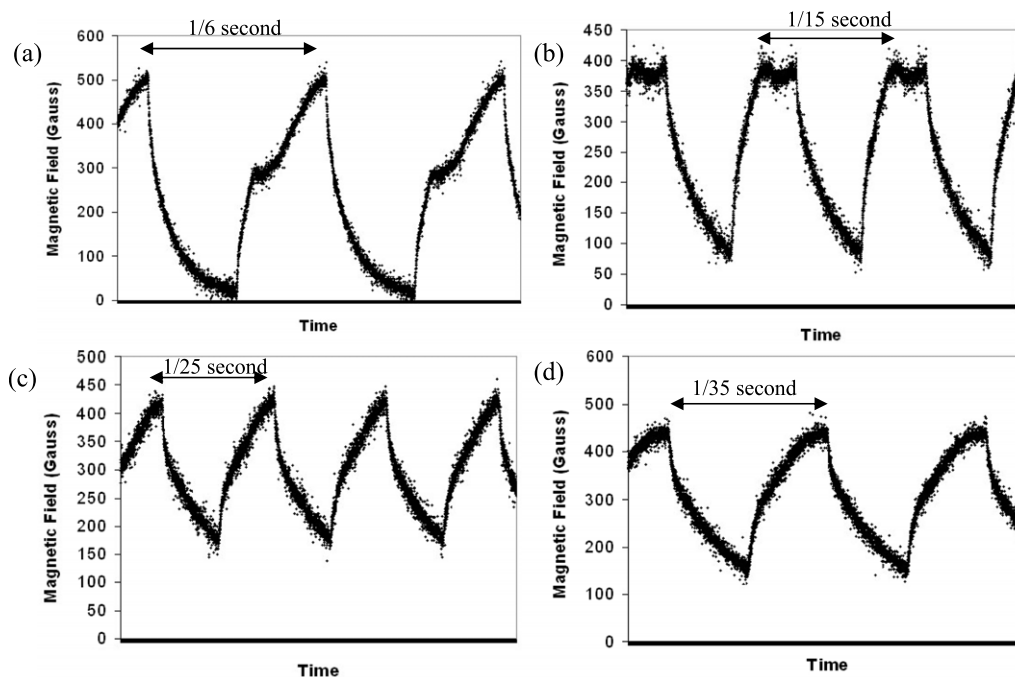
Figure 12. The magnetic field of the electromagnet measured at (a) 6 Hz, (b) 15 Hz, (c) 25 Hz and (d) 35 Hz.

system to increase the dynamic response of the active clutch. This revision improves the performance of the inchworm actuator up to a stroke speed of 65 mm s^{-1} at 14 Hz to lift a 3 kg subject. However, a robust and new design is needed for a stronger lifting force and faster stroke speed in the future.

High speed actuation of the inchworm actuator is one of the most important goals to achieve. The actuation speed is controlled by the dynamic responses of the FSMA composite, the clutch system and the electromagnet system. The responses of these three systems have to match each other in order to provide the maximum speed of actuation. As discussed previously, the dynamic responses of both the FSMA composite and the clutch system can be improved by increasing the stiffness of the composite and adding a spring to the clutch system, respectively. On the other hand, the dynamic response of the electromagnet system depends on how fast the magnetic flux can change in the soft iron yoke. As the rate change of flux in the yoke increases, the

eddy current effect becomes more significant, resulting in poor response of the electromagnet. The number of turns of the magnetic coil is another factor that influences the dynamic response of the electromagnet. Figure 12 shows the measured magnetic field near the armature of the electromagnet system of the inchworm actuator at various frequencies. At 6 Hz (figure 12(a)), the signals of the magnetic flux oscillate between 0 and 500 G. As the frequency increases (figures 12(b)–(d)), the residual field becomes higher at about 200 G. This means the FSMA composite still experiences magnetic gradient (force) when the composite finishes the stroke and starts to return. So this residual magnetic field will cause the FSMA composite to return to its initial position at slower speed. Therefore, the stroke of the oscillating FSMA composite will get smaller. This is one of the reasons why the speed (65 mm s^{-1}) of pushing the block at 7 Hz is almost the same as that at 14 Hz, as described in the experimental results of figure 8. In order to improve the electromagnet for higher

frequency usage, a laminated yoke has to be used to construct the electromagnet for the passage of the magnetic flux while minimizing the eddy current heating.

5. Summary

A prototype inchworm actuator based on a FSMA composite and hybrid mechanism was successfully designed and demonstrated. Each inchworm step is induced by the displacement of the FSMA composite via an active clutch system. A long stroke can be accumulated based on the duration of the oscillating FSMA composite driven by the electromagnetic driver. The hybrid mechanism is based on the stress-induced martensitic phase transformation produced by an applied magnetic field gradient, thus enhancing the displacement, as the stiffness of shape memory alloy reduces due to the martensitic phase transformation. The new inchworm actuator has proven to provide 30 N force at 65 mm s^{-1} stroke speed while the total stroke can be much longer if a longer central rod is available.

Acknowledgments

References

[1] Sugiyama M, Oshima R and Fujita F E 1986 Mechanism of FCC–FCT thermoelastic martensitic-transformation in Fe–Pd alloys *Trans. Japan Inst. Met.* **27** 719–30

[2] James R D and Wuttig W 1998 Magnetostriction of martensite *Phil. Mag.* A **77** 1273–99

[3] Kato H, Wada T, Liang Y, Tagawa T, Taya M and Mori T 2002 Martensite structure in polycrystalline Fe–Pd *Mater. Sci. Eng.* A **332** 134–9

[4] Liang Y, Kato H and Taya M 2006 Model calculation of 3D phase transformation diagram of ferromagnetic shape memory alloys *Mech. Mater.* **38** 564–70

[5] Wada T and Taya M 2002 Spring-based actuators *Proc. SPIE* **4699** 294–302

[6] Kusaka M and Taya M 2004 Design of ferromagnetic shape memory alloy composites *J. Compos. Mater.* **38** 1011–35

[7] Liang Y, Kuga Y and Taya M 2005 Design of membrane actuators based on ferromagnetic shape memory alloy composite for synthetic jet applications *Sensors Actuators* A **125** 512–8

[8] Galantea T, Frankb J, Bernardb J, Chen W, Lesieutre G A and Koopmannb G H 1998 Design, modeling, and performance of a high force piezoelectric inchworm motor *Proc. SPIE* **3329** 756–67

[9] Tenzer P E and Mrad R B 2004 A systematic procedure for the design of piezoelectric inchworm precision positioners *IEEE/ASME Trans. Mechatron.* **9** 427–35

[10] Le Letty R, Claeyssen F, Barillot F, Six M F and Bouchilloux P 1998 New linear Piezomotor for high force/precise positioning applications *The 1998 IEEE Industry Applications Conf., Thirty-Third IAS Annual Mtg* 1, pp 213–7

[11] Zhang B and Zhu Z 1997 Developing a linear piezomotor with nanometer resolution and high stiffness *IEEE Trans. Mechatron.* **2** 22–9

[12] May W G Jr 1975 Piezoelectric electromechanical translation apparatus *US Patent Specification* 3902084

[13] Salisbury S P, Waechter D F, Mrad R B, Prasad S E, Blacow R G and Yan B 2006 Design considerations for complementary inchworm actuators *IEEE/ASME Trans. Mechatron.* **11** 265–72

[14] Erismis M A, Neves H P, Puers R and Hoof C V 2004 A systematic procedure for the design of piezoelectric inchworm precision positioners *IEEE/ASME Trans. Mechatron.* **9** 427–35

[15] Kim J, Kim J D and Choi S B 2002 A hybrid inchworm linear motor *Mechatronics* **12** 525–42

[16] Vaughan M E 2001 The design, fabrication, and modeling of a piezoelectric linear motor *MS Thesis* Virginia Polytechnic Institute and State University

[17] Li J, Sedaghati R, Dargahi J and Waechter D 2005 Design and development of a new piezoelectric linear Inchworm actuator *Mechatronics* **15** 651–81

[18] Frank J, Koopmann G H, Chen W and Lesieutre G A 1999 Design and performance of a high force piezoelectric Inchworm motor *Proc. SPIE* **3668** 717–23

[19] Newton D, Garcia E and Horner G C 1998 A linear piezoelectric motor *Smart Mater. Struct.* **7** 295–304